JACS
JOURNAL OF THE AMERICAN CHEMICAL SOCIETY
pubs.acs.org/JACS
Article

Copper(III) Metallacyclopentadienes via Zirconocene Transfer and Reductive Elimination to an Isolable Phenanthrocyclobutadiene

Harrison M. Bergman, D. Dawson Beattie, Rex C. Handford, Elliot Rossomme, Benjamin A. Suslick, Martin Head-Gordon, Thomas R. Cundari,* Yi Liu,* and T. Don Tilley*

Cite This: *J. Am. Chem. Soc.* 2022, 144, 9853−9858
Read Online
ACCESS | Metrics & More | Article Recommendations | Supporting Information

ABSTRACT: Despite the widespread use of copper catalysis for the formation of C−C bonds, debate about the mechanism persists. Reductive elimination from Cu(III) is often invoked as a key step, yet examples of its direct observation from isolable complexes remain limited to only a few examples. Here, we demonstrate that incorporation of bulky mesityl (Mes) groups into the α-positions of a phenanthrene-appended zirconacyclopentadiene, $Cp_2Zr(2,5\text{-}Mes_2\text{-}phenanthro[9,10]C_4)$, enables efficient oxidative transmetalation to the corresponding, formal Cu(III) metallacyclopentadiene dimer. The dimer was quantitatively converted to a structurally analogous anionic monomer $[^nBu_4N]\{Cl_2Cu(2,5\text{-}Mes_2\text{-}phenanthro[9,10]C_4)\}$ upon treatment with $[^nBu_4N][Cl]$. Both metallacycles undergo quantitative reductive elimination upon heating to generate phenanthrocyclobutadiene and a Cu(I) species. Due to the steric protection provided by the mesityl groups, this cyclobutadiene was isolated and thoroughly characterized to reveal antiaromaticity comparable to that of free cyclobutadiene, which imbues it with a small highest occupied molecular orbital−lowest unoccupied molecular orbital energy gap of 1.85 eV and accessible reduced and oxidized electronic states.

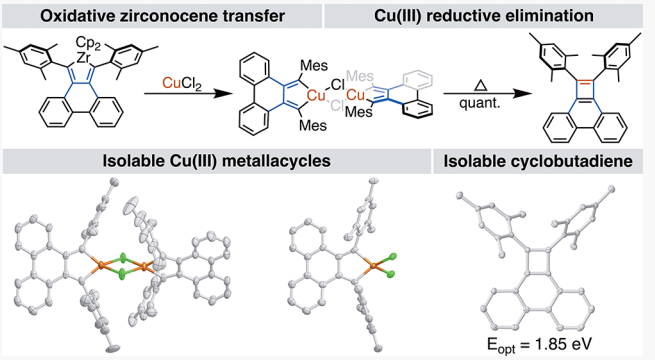

INTRODUCTION

Copper catalysis is ubiquitous in organic synthesis, where it has become one of the most powerful strategies for the formation of C−C and C-heteroatom bonds.[1−3] Reductive elimination from a formal Cu(III) species is often invoked as a key step in these transformations,[4−6] yet its direct observation from well-defined complexes is rare due in large part to the difficulty of isolating these highly reactive species.[7−10] Notable examples include Xi and co-workers' observation of $C_{sp^2}-C_{sp^2}$ bond formation in reactions of an anionic Cu(III) spirocycle with electrophiles,[11] Shen's synthesis of a neutral Cu(III) complex that undergoes $C_{sp^3}-C_{sp^3}$ bond formation upon gentle heating,[12] and Liu's trifluoromethylation via isolated, anionic Cu(III) complexes (Figure 1a).[13] While these examples affirm the competency of formal Cu(III) for high yielding reductive eliminations to form C−C bonds, the scope of transformations is still extremely limited.

Zirconacyclopentadienes provide a platform for exploring diverse reactivity from high valent copper species due to their tunable structures and rich, well-developed copper transmetalation chemistry.[14] Zirconacycles mediate a wide range of C−C bond forming reactions including homocouplings, cross-couplings, and formal cycloadditions, many of which occur through transmetalation to ill-defined copper intermediates.[15] Although there is speculation that these transmetalations involve generation of a cupracyclopentadiene,[16] such intermediates have not been directly observed. Several transmetalations with Cu(II) or Cu(I) and an oxidant are of particular interest as they generate transient cyclobutadienes (CBDs), likely via reductive elimination from a high valent copper species. An early example is Xi's discovery of cyclooctatetraene formation upon treatment of the zirconacycle with CuCl and benzoquinone, proposed to occur through a transient CBD (Figure 1b).[17] This pathway is supported by Hong's observation of benzocyclobutadiene dimers under similar conditions[18] and by Xie's synthesis of a persistent carboranyl-cyclobutene via treatment of a zirconacycle precursor with $CuCl_2$.[19,20]

CBDs are themselves fundamentally interesting synthetic targets as prototypical examples of antiaromaticity, with unique structural,[21] chemical,[22] and electronic properties.[23] Fusion to larger ring systems stabilizes the CBD and can result in low-bandgap polycyclic aromatic hydrocarbons;[24] however, fusion

Received: March 8, 2022
Published: May 23, 2022

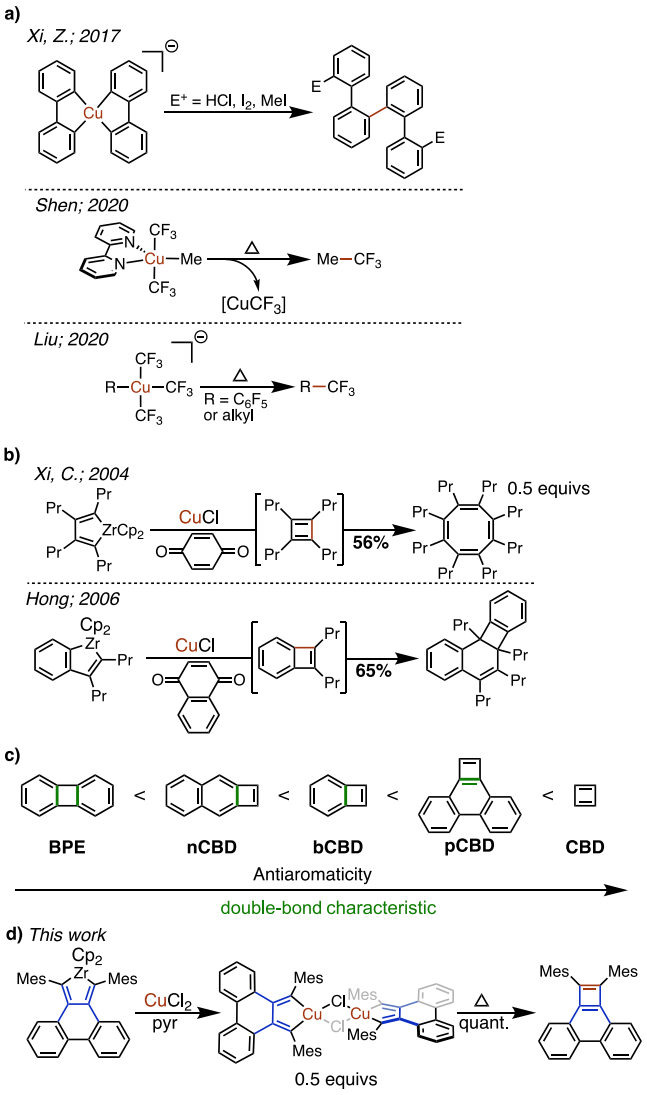

Figure 1. (a) Examples of C−C bond formation via reductive elimination from isolable Cu(III) complexes; (b) examples of purported and observed cyclobutadienoid formation from zirconacyclopentadienes; (c) depiction of relative antiaromaticity of CBDs appended to different common polycyclic aromatic hydrocarbons; and (d) this work.

to an aromatic system also decreases the antiaromaticity of the CBD by delocalizing the 4π electrons across a larger conjugated system (Figure 1c). In these fused ring systems, the double-bond characteristic of the shared edge determines the degree of antiaromaticity (and consequently the instability) of the PAH−CBD conjugate.[25] Thus, whereas CBDs appended to highly delocalized ring systems (e.g., benzene and naphthalene) have been isolated,[26−29] phenanthrene-fused CBDs have proven elusive due to the highly localized double bond on the central phenanthrene ring.[30−32] Access to fused ring PAH−CBDs has also been severely limited by the lack of appropriate synthetic methodologies.

Here, we describe the isolation of two formal Cu(III) metallacyclopentadienes from zirconacycles and their quantitative reductive elimination to the persistent phenanthrocyclobutadiene (pCBD) shown in Figure 1d. Steric stabilization of the high-valent copper intermediates provides mechanistic insights into both the unusual oxidative transmetalation of a zirconacycle to a high-valent cupracycle and the Cu(III)−Cu(I) reductive elimination that generates the pCBD. This pCBD displays high antiaromatic characteristic and a low optical highest occupied molecular orbital (HOMO)−lowest unoccupied molecular orbital (LUMO) energy gap of 1.85 eV.

RESULTS AND DISCUSSION

The initial interest in this system came from the observation that zirconacycle **1a** generated COT **2** in a good yield upon treatment with $CuCl_2$, suggesting the formation of a transient CBD similar to those observed by Xi (Scheme 1). It therefore seemed that bulky aryl substituents at the two and five positions of the zirconacycle might facilitate isolation of one or more of these transient species. To this end, mesityl groups were introduced to zirconacycle **1b**, generated from the appropriate diyne in the presence of $Cp_2Zr(Me_3SiC{\equiv}CSiMe_3)$(pyr) at 60 °C in 89% yield (Scheme S1). Subsequent treatment of the in situ generated **1b** with $CuCl_2$ gave a new deep-red species, isolated and characterized by X-ray crystallography as the formal Cu(III) metallacyclopentadiene **3-dim**. Further investigation showed that the *isolated* zirconacycle **1b** did not undergo this clean transformation, but addition of pyridine to the reaction mixture provided **3-dim** in 87% yield (Page S5). The notably lower isolated yield (40%) is due to the difficulty in separating **3-dim** from the Cp_2ZrCl_2 side product, which was accomplished by trituration with

Scheme 1. Synthesis of Cu(III) Metallacyclopentadienes and pCBD

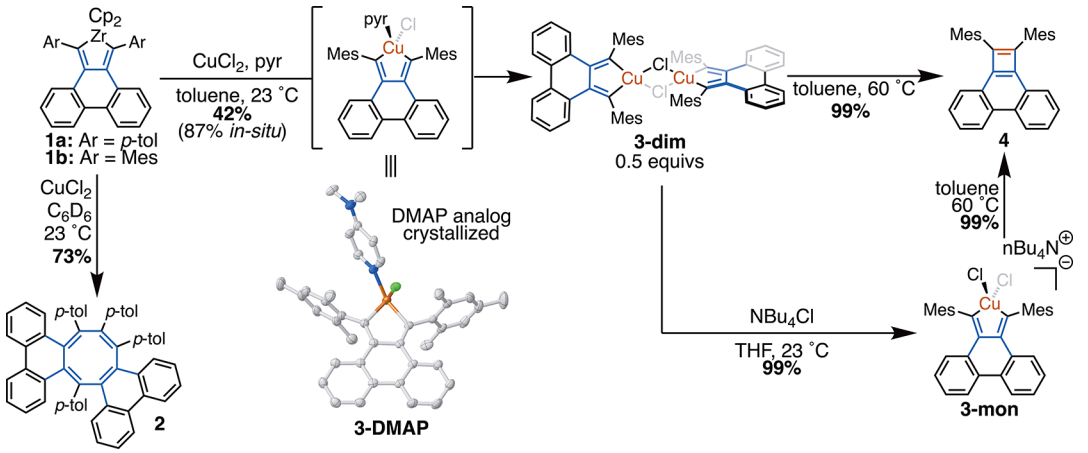

https://doi.org/10.1021/jacs.2c02581
J. Am. Chem. Soc. 2022, 144, 9853−9858

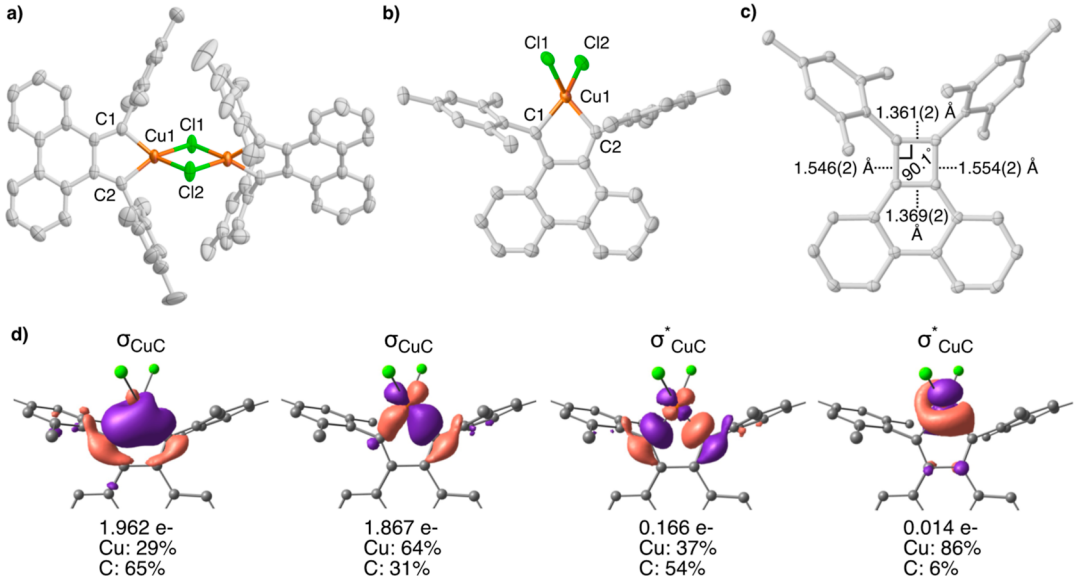

Figure 2. Structural analysis of key compounds. Crystallographic solid-state molecular structures (a) **3-dim**; (b) **3-mon**; and (c) **4**, with key bond lengths and angles indicated. All hydrogen atoms have been omitted for clarity, and thermal ellipsoids are drawn at 50% probability. (d) MCSCF analysis of **3-mon** frontier orbitals with NOONs indicated; the orbital percentages are determined from a Mulliken population of the active space natural orbitals.

acetonitrile. The surprising formation of the formal Cu(III) metallacycle is proposed to occur via oxidation of a Cu(II) species by $CuCl_2$, and this is supported by the marked increase in yield from 42% with stoichiometric $CuCl_2$ to 87% upon addition of 3 equiv (Page S5), as well as by the formation of copper mirror during the reaction.

To better understand the role of pyridine in facilitating this unusual transformation, the interaction of the more strongly donating 4-dimethylaminopyridine (DMAP) with the isolated dimer **3-dim** in benzene-d_6 solution was examined by ^{1}H NMR spectroscopy (Figure S1). The addition of 2.0 equiv of DMAP resulted in marked shifts of all resonances associated with the dimer and extremely broadened DMAP resonances. Additional DMAP (3.2 and 4.4 equiv) caused further shifting of the resonances but did not result in the emergence of two sets of DMAP peaks at 23 °C, suggesting dynamic exchange in solution. Despite the apparently dynamic nature of the DMAP coordination, the crystals of the resulting complex **3-DMAP** were grown by vapor diffusion of pentane into an Et_2O solution containing excess DMAP. An X-ray diffraction analysis revealed a monomeric molecular structure, indicating cleavage of the dimer by DMAP. This suggests that the initial product of transmetalation is the monomeric pyridine adduct, which then converts to **3-dim** upon removal of pyridine under vacuum.

A related monomer that does not appear to undergo a dynamic process in solution, **3-mon**, was prepared by the quantitative reaction of **3-dim** with [^{n}Bu$_4$N]Cl in tetrahydrofuran (THF). In contrast to the DMAP adduct, **3-mon** displays sharp resonances in its ^{1}H NMR spectrum that do not shift or broaden upon addition of excess chloride.

The crystallographically determined molecular structures of **3-dim** and **3-mon** reveal similar pseudo-tetrahedral coordination environments at copper, with average Cu−C_{sp^2} bond distances of 1.933(7) and 1.940(3) Å and τ_4' values of 0.74 and 0.72, respectively (Figure 2a,b). These Cu−C distances are slightly shorter than the Cu−C_{aryl} bond lengths of Xi's spiro Cu(III) complexes [1.952(3)−1.968(3) Å][11] and the Cu−C_{sp^3} bond length of Shi's neutral five-coordinate Cu(III) complex [1.956(8) Å].[12] Particularly notable is the pseudo-tetrahedral coordination environment, which is distinctly different from the distorted square-planar geometries of both Xi's spirocycle and Liu's anionic Cu(III) complexes.[13]

Both **3-dim** and **3-mon** undergo rapid, quantitative reductive elimination to CBD **4** at 60 °C. Compound **4** is diamagnetic and displays the same symmetry as the metallacycles by ^{1}H NMR spectroscopy. Single crystals were grown by slow evaporation of a 50:50 pentane/hexamethyldisiloxane solution, and X-ray structure determination confirmed **4** to be a pCBD (Figure 2c).

Multiconfiguration SCF calculations were performed on the DFT-optimized coordinates for **3-mon**. The natural orbitals exhibiting a dominant σ_{CuC} characteristic are plotted in Figure 2d. Several points are of interest with respect to the observed reactivity of this key intermediate. First, the orbitals for the Cu−C bonds of **3-mon** are surprisingly covalent in nature with little (ca. 7%) characteristics from orbitals on other atoms. The in-phase combination of the σ_{CuC} natural orbitals is ∼2:1 copper to carbon in nature, while the polarity of the out-of-phase combination is reversed. Second, the in-phase pair of $\sigma_{CuC}/\sigma^*_{CuC}$ orbitals is well described at the single determinant level [natural orbital occupation numbers (NOONs) = 1.96 and 0.01 e$^-$, respectively]; the out-of-phase pair shows a more multireference characteristic, NOONs = 1.87 and 0.17 e$^-$ for σ_{CuC} and σ^*_{CuC}, respectively, albeit still with a dominant single-determinant characteristic. Taken together, the MCSCF-derived frontier orbitals are consistent with a Cu(III)-based cyclopentadiene ideally set up for reductive elimination to form **4** and a Cu(I) complex. As noted below, butylated hydroxytoluene (BHT) did not inhibit the reductive elimination, which is consistent with the limited diradical characteristic of **3-mon**.

The molecular structure of **4** is consistent with a high degree of antiaromatic character, with significant bond length alternation and C−C bond lengths that closely match the common values for single [1.546(2) and 1.554(2) Å] and

https://doi.org/10.1021/jacs.2c02581
J. Am. Chem. Soc. 2022, 144, 9853−9858

double [1.361(2) and 1.369(2) Å] bonds. This suggests a closed-shell singlet ground state as observed in the parent CBD.[22] The observed bond shift isomer places the double bonds on the edge fused to phenanthrene and the opposite edge.

NICS-XY calculations on truncated **4** (pCBD) corroborate its large antiaromatic characteristic in reference to the PAH−CBDs illustrated in Figure 1. Each compound was scanned linearly through its CBD ring and all adjacent rings at a height of 1.7 Å (see Page S21), and values at the center of each CBD ring are summarized in Table 1. These results show that the CBD ring of **4** displays a significantly larger paratropic ring current than other benzo-fused CBDs and even the parent CBD itself. As paratropicity is not a direct measure of antiaromaticity, this does not suggest that **4** is more antiaromatic than CBD, but in concert with the crystallographic data supports the claim that the fusion of CBD to phenanthrene does not greatly attenuate its antiaromaticity.

Table 1. Summary of Maximum $NICS_{ZZ}$ Values for Common PAH−CBD Motifs

cmpd	BPE	nCBD	bCBD	**pCBD**	CBD
$NICS_{ZZ}$ (ppm)	7.45	9.90	13.21	**19.51**	16.77

As expected for a highly antiaromatic species, CBD **4** displays a low optical and electrochemical HOMO−LUMO energy gap. The UV−vis spectrum of a 4.15×10^{-5} M solution in benzene illustrates broad absorption across the visible region, with two major absorption features at 434 and 451 nm, a shoulder at 528 nm, and a broad tail that extends past 730 nm (Figure 3a). This indicates an optical HOMO−LUMO energy gap of 1.85 eV. Cyclic voltammetry of **4** in THF reveals a chemically reversible oxidation event at 0.24 V, and two chemically reversible reduction events at −2.19 and −2.67 V, corresponding to an electrochemical HOMO−LUMO energy gap of 2.35 eV (Figure 3b).

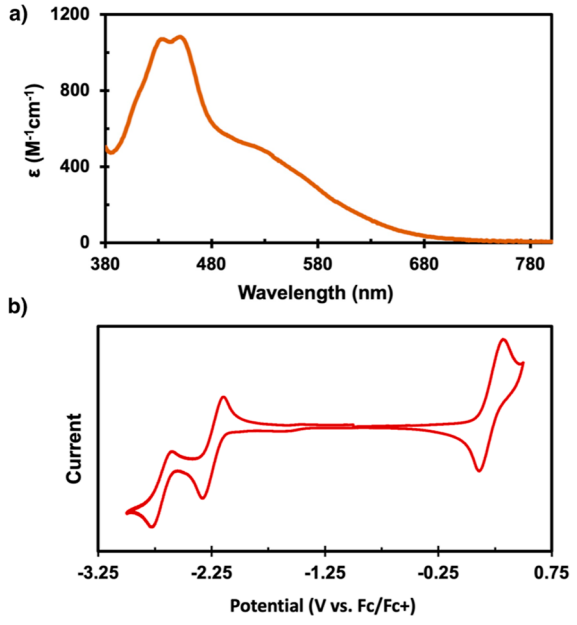

Figure 3. Electronic characterization of **4**. (a) UV−vis spectroscopy at 3.25×10^{-6} M in benzene. Inset displayed at 10× magnification for visualization of the absorption edge; (b) cyclic voltammogram of a 0.2 mM solution of **4** in THF with 0.1 M $[^nBu_4N][PF_6]$ as the supporting electrolyte. Scan rate: 100 mV/s.

Due to the efficiency of the rare reductive elimination reaction described above, further mechanistic understanding was sought. First, the reductive elimination of **3-dim** was allowed to proceed in the presence of 1,3-bis(2,6-diisopropylphenyl)imidazol-2-ylidene (IPr) as a trap for CuCl (Scheme S3). This reaction quantitatively gave **4** and (IPr)CuCl, confirming that a Cu(I) species is formed upon reductive elimination. The elimination reaction is not affected by addition of 2.0 equiv of BHT as a potential radical trap, which is consistent with the absence of radical intermediates (Scheme S4). These results provide strong support for a two-electron, formally Cu(III) to Cu(I) reductive elimination rather than a more complex sequence of one-electron redox events.

The kinetics of this process were studied by monitoring the ^{1}H NMR spectra of a solution of **3-dim** in benzene-d_6 as the temperature was raised from 48 to 60 °C (Figure 4a). The reductive elimination was found to be first order in consumption of the dimer, and an Eyring analysis provided the activation parameters $\Delta H^{\ddagger} = 23(1)$ kcal/mol and $\Delta S^{\ddagger} = 20(1)$ cal/(mol K) (Figure 4b).

Due to the potential mechanistic complexity of reductive elimination from the dimer, a similar analysis was applied to **3-mon** in benzene-d_6 between 55 and 65 °C. In this case, the kinetic data also indicate first-order dependence on starting material consumption (Figure 4c), with $\Delta H^{\ddagger} = 24(2)$ kcal/mol and $\Delta S^{\ddagger} = 22(2)$ cal/(mol K). The large entropy of activation suggests a dissociative mechanism, whereby the chloride anion dissociates prior to reductive elimination. To further explore this possibility, the kinetics were evaluated for the reaction in the polar solvent THF-d_8 at 55 °C (Figure S2). Though chloride dissociation might be expected to be more favorable under these conditions, the observed rate constant ($k_{obs} = 4.5(2) \times 10^{-4}$ s^{-1}) is nearly identical to that found for benzene-d_6 solvent, $k_{obs} = 4.9(4) \times 10^{-4}$ s^{-1}. In addition, the reductive elimination from **3-mon** proceeds at the same rate ($k_{obs} = 5.1(3) \times 10^{-4}$ s^{-1}) in THF solvent in the presence of a 10-fold excess of tetrabutylammonium chloride. These experiments indicate that dissociation of chloride does not precede reductive elimination despite the high entropy of activation. Thus, the most likely mechanism involves direct elimination from complex **3-mon** to generate **4** and $[^nBu_4N][CuCl_2]$ as a byproduct. Given the similar activation parameters for **3-mon** and **3-dim**, it is possible that the rate-determining step for reductive elimination from **3-dim** occurs directly from the dimer, rather than being preceded by dissociation into two monomeric complexes. Notably, both complexes efficiently undergo reductive elimination in the solid state at 60 °C, further supporting the idea that no prior dissociation occurs.

CONCLUSIONS

In conclusion, the results described above highlight several unusual patterns of reactivity that have implications across diverse areas of synthetic chemistry. The unusual oxidative transmetalation of zirconacyclopentadienes observed in the formation of Cu(III) metallacyclopentadienes represents a conceptually new strategy for accessing isolable, highly oxidized metallacycles. The facile Cu(III)−Cu(I) reductive elimination to generate CBDs illustrates a particularly challenging C−C bond formation, and its demonstration with an isolated Cu(III) species underscores the synthetic

https://doi.org/10.1021/jacs.2c02581
J. Am. Chem. Soc. 2022, 144, 9853−9858

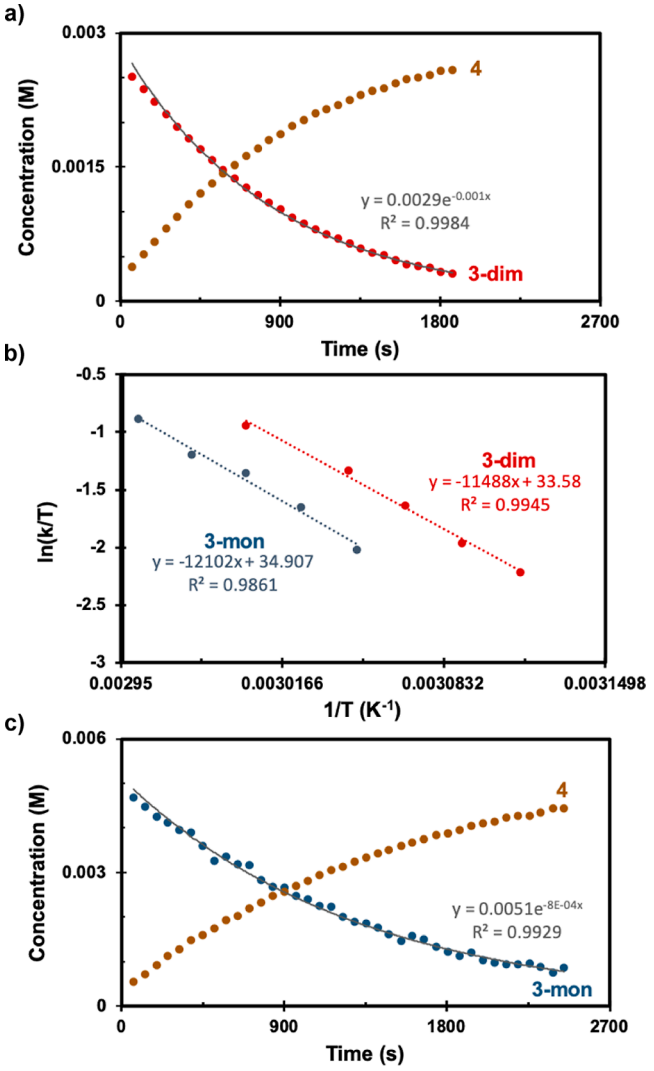

Figure 4. Kinetics of reductive elimination of **3-dim** and **3-mon**. (a) Representative kinetic profile of **3-dim** reductive elimination at 60 °C in C_6D_6; (b) Eyring analysis of the temperature dependence of rate of reductive elimination for **3-dim** (in red) and **3-mon** (in blue); and (c) representative kinetic profile of **3-mon** reductive elimination at 60 °C in C_6D_6.

utility of Cu(III). This transmetalation−reductive elimination sequence also presents a new strategy for the efficient synthesis of PAH−CBD conjugates, as exemplified by the isolation and structural characterization of the previously unobserved pCBD, whose broad absorption, small HOMO−LUMO energy gap, and well-defined electrochemistry suggest intriguing applications in organic electronic materials. Expansion of this strategy to other PAH−CBDs is ongoing in this laboratory.

■ ASSOCIATED CONTENT

Supporting Information

The Supporting Information is available free of charge at https://pubs.acs.org/doi/10.1021/jacs.2c02581.

Experimental procedures and characterization data for all new compounds (PDF)

Accession Codes

CCDC 2145426−2145429 contain the supplementary crystallographic data for this paper. These data can be obtained free of charge via www.ccdc.cam.ac.uk/data_request/cif, or by emailing data_request@ccdc.cam.ac.uk, or by contacting The Cambridge Crystallographic Data Centre, 12 Union Road, Cambridge CB2 1EZ, UK; fax: +44 1223 336033.

■ AUTHOR INFORMATION

Corresponding Authors

Thomas R. Cundari − *Department of Chemistry, Center for Advanced Scientific Computing and Modeling (CASCaM), University of North Texas, Denton, Texas 76203, United States;* orcid.org/0000-0003-1822-6473; Email: t@unt.edu

Yi Liu − *Molecular Foundry, Lawrence Berkeley National Laboratory, Berkeley, California 94720, United States;* orcid.org/0000-0002-3954-6102; Email: yliu@lbl.gov

T. Don Tilley − *Department of Chemistry, University of California, Berkeley, Berkeley, California 94720, United States;* orcid.org/0000-0002-6671-9099; Email: tdtilley@berkeley.edu

Authors

Harrison M. Bergman − *Department of Chemistry, University of California, Berkeley, Berkeley, California 94720, United States;* orcid.org/0000-0001-6482-2837

D. Dawson Beattie − *Department of Chemistry, University of California, Berkeley, Berkeley, California 94720, United States;* orcid.org/0000-0002-7909-2416

Rex C. Handford − *Department of Chemistry, University of California, Berkeley, Berkeley, California 94720, United States;* orcid.org/0000-0002-3693-1697

Elliot Rossomme − *Department of Chemistry, University of California, Berkeley, Berkeley, California 94720, United States; Kenneth S. Pitzer Center for Theoretical Chemistry, University of California, Berkeley, California 94720, United States; Chemical Sciences Division, Lawrence Berkeley National Laboratory, Berkeley, California 94720, United States*

Benjamin A. Suslick − *Department of Chemistry, University of California, Berkeley, Berkeley, California 94720, United States;* orcid.org/0000-0002-6499-3625

Martin Head-Gordon − *Department of Chemistry, University of California, Berkeley, Berkeley, California 94720, United States; Kenneth S. Pitzer Center for Theoretical Chemistry, University of California, Berkeley, California 94720, United States; Chemical Sciences Division, Lawrence Berkeley National Laboratory, Berkeley, California 94720, United States;* orcid.org/0000-0002-4309-6669

Complete contact information is available at: https://pubs.acs.org/10.1021/jacs.2c02581

Funding

This work was funded by the National Science Foundation under grant no. CHE-2103696.

Notes

The authors declare no competing financial interest.

■ ACKNOWLEDGMENTS

Work performed at the Molecular Foundry was supported by the Office of Science, Office of Basic Energy Sciences, US Department of Energy under contract no. DE-AC02-05CH11231. The initial computational work was performed at the UC Berkeley Molecular Graphics and Computation

Facility (MGCF), which is supported by the National Institute of Health (grant no. NIH S10OD023532), and the authors thank Dr. Dave Small and Dr. Kathy Durkin for their assistance with these calculations. The authors thank Dr. Hasan Celik for assistance with NMR spectroscopy. The authors thank Gavin R. Kiel for useful discussions, Rebecca Khoo for preliminary help with crystallography, and Laurent Severy for help with cyclic voltammetry. Crystallographic analysis of **3-dim**, **3-DMAP**, and **3-mon** was performed at The Advanced Light Source, which is supported by the Director, Office of Science, Office of Basic Energy Sciences, U.S. Department of Energy under contract no. DE-AC02-05CH11231. Crystallographic analysis of **4** was performed at UC Berkeley CheXray facility, which is supported by the NIH Shared Instrumentation grant S10-RR027172. The CIF files can also be obtained free of charge from the Cambridge Crystallographic Data Centre under reference numbers 2145426−2145429.

REFERENCES

(1) Gopinathan, A.; Saranya, S. *Copper Catalysis in Organic Synthesis*, 1st ed.; John Wiley and Sons, 2020.
(2) Lin, H.; Sun, D. Recent Synthetic Developments and Applications of the Ullmann Reaction. A Review. *Org. Prep. Proced. Int.* **2013**, *45*, 341−394.
(3) Sambiagio, C.; Marsden, S. P.; Blacker, A. J.; McGowan, P. C. Copper Catalyzed Ullmann Type Chemistry: from Mechanistic Aspects to Modern Development. *Chem. Soc. Rev.* **2014**, *43*, 3525−3550.
(4) Li, S.-J.; Lan, Y.; Lan, Y. Is Cu(III) a Necessary Intermediate in Cu-Mediated Coupling Reactions? A Mechanistic Point of View. *Chem. Commun.* **2020**, *56*, 6609−6619.
(5) Casitas, A.; Ribas, X. The Role of Organometallic Copper(III) Complexes in Homogeneous Catalysis. *Chem. Sci.* **2013**, *4*, 2301−2318.
(6) DiMucci, I. M.; Lukens, J. T.; Chatterjee, S.; Carsch, K. M.; Titus, C. J.; Lee, S. J.; Nordlund, D.; Betley, T. A.; MacMillan, S. N.; Lancaster, K. M. The Myth of d^8 Copper(III). *J. Am. Chem. Soc.* **2019**, *141*, 18508−18520.
(7) King, A. E.; Huffman, L. M.; Casitas, A.; Costas, M.; Ribas, X.; Stahl, S. S. Copper-Catalyzed Aerobic Oxidative Functionalization of an Arene C-H Bond: Evidence for an Aryl-Copper(III) Intermediate. *J. Am. Chem. Soc.* **2010**, *132*, 12068−12073.
(8) Ribas, X.; Jackson, D. A.; Donnadieu, B.; MahÌa, J.; Parella, T.; Hedman, B.; Hodgson, K. O.; Llobet, A.; Daniel Stack, T. P.; Llobet, A.; et al. Aryl C-H Activation by CuII To Form an Organometallic Aryl−CuIII Species: A Novel Twist on Copper Disproportionation†. *Angew. Chem., Int. Ed.* **2002**, *41*, 2991.
(9) Casitas, A.; King, A. E.; Parella, T.; Costas, M.; Stahl, S. S.; Ribas, X. Direct Observation of Cu^{I}/Cu^{III} Redox Steps Relevant to Ullmann-Type Coupling Reactions. *Chem. Sci.* **2010**, *1*, 326−330.
(10) Yao, B.; Wang, D.-X.; Huang, Z.-T.; Wang, M.-X. Room Temperature Aerobic Formation of a Stable Aryl-Cu(III)Complex and its Reactions with Nucleophiles: Highly Efficient and Diverse Arene C-H Functionalizations of Azacalix[1]arene[3]pyridine. *Chem. Commun.* **2009**, 2899−2901.
(11) Liu, L.; Zhu, M.; Yu, H.-T.; Zhang, W.-X.; Xi, Z. Organocopper(III) Spiro Complexes: Synthesis, Structural Characterization, and Redox Transformation. *J. Am. Chem. Soc.* **2017**, *139*, 13688−13691.
(12) Liu, S.; Liu, H.; Liu, S.; Lu, Z.; Lu, C.; Leng, X.; Lan, Y.; Shen, Q.; Shen, Q. C(Sp3)-CF3Reductive Elimination from a Five-Coordinate Neutral Copper(III) Complex. *J. Am. Chem. Soc.* **2020**, *142*, 9785−9791.
(13) Paeth, M.; Tyndall, S. B.; Chen, L.-Y.; Hong, J.-C.; Carson, W. P.; Liu, X.; Sun, X.; Liu, J.; Yang, K.; Hale, E. M.; Tierney, D. L.; Liu, B.; Cao, Z.; Cheng, M.-J.; Goddard, W. A.; Liu, W. Csp3-Csp3 Bond-Forming Reductive Elimination from Well-Defined Copper(III) Complexes. *J. Am. Chem. Soc.* **2019**, *141*, 3153−3159.
(14) Yan, X.; Xi, C. Conversion of Zirconacyclopentadienes into Metalloles: Fagan−Nugent Reaction and Beyond. *Acc. Chem. Res.* **2015**, *48*, 935−946.
(15) Kotora, M.; Xi, Z.; Takahashi, T. Copper-Catalyzed or Mediated Carbon-Carbon Bond Formation Reactions of Zirconacycles and Alkenylzirconocenes. *J. Synth. Org. Chem., Jpn.* **1997**, *55*, 958−969.
(16) Liu, L.; Zhu, M.; Yu, H.-T.; Zhang, W.-X.; Xi, Z. Formation of a Hexanuclear Octatetraenyl Organocopper(I) Aggregate via Oxidation of Spiro Butadienyl Organocuprate. *Organometallics* **2018**, *37*, 845.
(17) Chen, C.; Xi, C.; Lai, C.; Wang, R.; Hong, X. Coupling Reactions of 1,4-Dicuprio-1,3-Dienes: Formation of Carbocycles. *Eur. J. Org. Chem.* **2004**, *2004*, 647−650.
(18) Chen, C.; Xi, C.; Liu, Y.; Hong, X. Generation of Benzocyclobutadiene Derivatives from Zirconaindene Derivatives. *J. Org. Chem.* **2006**, *71*, 5373−5376.
(19) Ren, S.; Chan, H.-S.; Xie, Z. Synthesis, Structure, and Reactivity of Sirconacyclopentene Incorporating a Carboranyl Unit. *J. Am. Chem. Soc.* **2009**, *131*, 3862−3863.
(20) Yuan, Y.; Ren, S.; Qiu, Z.; Wang, S.; Xie, Z.; Kong, S.-H. Synthesis of Carborane-Fused Cyclobutenes and Cyclobutanes. *Sci. China: Chem.* **2014**, *57*, 1157−1163.
(21) Legrand, Y.-M.; van der Lee, A.; Barboiu, M. Single-Crystal X-Ray Structure of 1,3-Dimethylcyclobutadiene by Confinement in a Crystalline Matrix. *Science* **2010**, *329*, 299−302.
(22) Inagaki, Y.; Nakamoto, M.; Sekiguchi, A. A Diels−Alder Super Diene Breaking Benzene into C2H2 and C4H4 Units. *Nat. Commun.* **2014**, *5*, 3018.
(23) Bally, T. Cyclobutadiene: The Antiaromatic Paradigm? *Angew. Chem., Int. Ed.* **2006**, *45*, 6616−6619.
(24) Toda, F.; Garratt, P. Four-Membered Ring Compounds Containing Bis(Methylene)Cyclobutene or Tetrakis(Methylene)-Cyclobutane Moieties. Benzocyclobutadiene, Benzodicyclobutadiene, Biphenylene, and Related Compounds. *Chem. Rev.* **2002**, *92*, 1685−1707.
(25) Frederickson, C. K.; Zakharov, L. N.; Haley, M. M. Modulating Paratropicity Strength in Diareno-Fused Antiaromatics. *J. Am. Chem. Soc.* **2016**, *138*, 16827−16838.
(26) Toda, F.; Ohi, M. Isolation of a Tricyclo[6,2,0,02,5]Deca-1,3,5,7,9-Pentaene. *J. Chem. Soc., Chem. Commun.* **1975**, *13*, 506.
(27) Straub, H. Stabile Derivate Des 3,4,5,6-Tetramethylbenzocyclobutadiens. *Justus Liebigs Ann. Chem.* **1978**, *1978*, 1675−1701.
(28) Winter, W.; Straub, H. Molecular Structure of a Benzocyclobutadiene. *Angew. Chem., Int. Ed. Engl.* **1978**, *17*, 127−128.
(29) Barker, J. E.; Kodama, T.; Song, M. K.; Frederickson, C. K.; Jousselin-Oba, T.; Zakharov, L. N.; Marrot, J.; Frigoli, M.; Johnson, R. P.; Haley, M. M. Serendipitous Rediscovery of the Facile Cyclization of Z,Z-3,5-Octadiene-1,7-Diyne Derivatives to Afford Stable, Substituted Naphthocyclobutadienes. *Chempluschem* **2019**, *84*, 665−672.
(30) Miyamoto, T.; Odaira, Y. The Reaction of Phenanthro[ζ]-Iicyclobutadiene. *Tetrahedron Lett.* **1973**, *14*, 43−46.
(31) Miyamoto, T.; Tanaka, S.; Odaira, Y.; Cava, M. P.; Hwang, B.; Van, J. P. Synthesis of Tricarbonylcyclobuta[/]Phenanthreneiron. *J. Am. Chem. Soc., Perkin Trans. 1* **1973**, 138.
(32) Cava, M. P.; Mangold, D. 1,2-Diphenylphenanthro[1]-Cyclobutadiene: A Highly Unstable Condensed Aromatic Cyclobutadiene. *Tetrahedron Lett.* **1964**, *5*, 1751−1754.

https://doi.org/10.1021/jacs.2c02581
J. Am. Chem. Soc. 2022, 144, 9853−9858